Mon. Not. R. Astron. Soc. **374,** L24–L28 (2007) doi:10.1111/j.1745-3933.2006.00257.x

Cosmic microwave background anisotropies from outflows in Lyman break galaxies

Daniel Babich★† and Abraham Loeb★

Astronomy Department, Harvard University, 60 Garden Street, Cambridge, MA 02138, USA

Accepted 2006 October 13. Received 2006 October 11; in original form 2006 September 18

ABSTRACT

Thomson scattering of the cosmic microwave background (CMB) on moving electrons in the outflows of Lyman break galaxies (LBGs) at redshifts 2–8 contributes to the small-scale CMB anisotropies. The net effect produced by each outflow depends on its level of deviation from spherical symmetry, caused either by an anisotropic energy injection from the nuclear starburst or quasar activity, or by an inhomogeneous intergalactic environment. We find that for plausible outflow parameters consistent with spectroscopic observations of LBGs, the induced CMB anisotropies on arcminute scales reach up to $\sim$1 μK, comparable to the level produced during the epoch of reionization.

Key words: galaxies: high-redshift – cosmic microwave background.

1 INTRODUCTION

Several experiments to observe the cosmic microwave background (CMB) anisotropies on arcminute scales are currently, or will soon be, underway (Kosowsky 2003; Ruhl et al. 2004; Lo et al. 2005). These experiments plan to measure the CMB power spectrum for a spherical harmonic multipole index of $10^3 \leqslant \ell \leqslant 10^4$ at several frequencies centred around the thermal Sunyaev–Zel'dovich null of 217 GHz. Photon diffusion damps the CMB anisotropies on these small scales during cosmological recombination at redshift $z \sim 10^3$ (Silk 1968), and so any observed signal must originate at much lower redshifts. Indeed, the above experiments plan to constrain the epoch of reionization and the growth of structure in the low-redshift Universe (Zahn et al. 2005).

The primary physical mechanism which is responsible for the small-scale CMB anisotropies is Thomson scattering of CMB photons off moving electrons. Any peculiar velocity induces a Doppler anisotropy of the scattered radiation along the direction of motion. This accounts for the CMB anisotropies produced by the peculiar velocities of clusters (the so-called *kinetic Sunyaev–Zel'dovich effect*) (Zel'dovich & Sunyaev 1980), by peculiar velocities of linear overdensities in the intergalactic medium (the so-called *Ostriker–Vishniac effect*) (Ostriker & Vishniac 1986; Vishniac 1987) and by the peculiar velocities of the fluctuations in the ionization fraction during patchy reionization (Gruzinov & Hu 1998).

In this Letter we examine the contribution of outflows in Lyman break galaxies (LBGs) to the small-scale CMB anisotropies. LBGs are believed to be the ancestors of present-day luminous elliptical galaxies. They are observed to produce gas outflows with velocities of several hundred km s^{-1} (see Giavalisco 2002 for a comprehensive review). In contrast with the traditional kinetic Sunyaev–Zel'dovich effect where the bulk velocity of the virialized gas is responsible for the induced CMB anisotropy, we focus here on the Doppler effect of the outflowing gas and ignore any bulk motion of the LBG as a whole (which produced a smaller effect at the redshifts of interest). This bulk effect is included in standard calculations of the non-linear generalization of the Ostiker–Vishniac effect (Hu 2000).

The contribution from a single LBG to the fractional temperature fluctuation of the CMB can be expressed as

$$\frac{\Delta T}{T} = -\int \mathrm{d}l \sigma_{\mathrm{T}} n_{\mathrm{e}} \frac{\hat{\boldsymbol{n}} \cdot \boldsymbol{v}}{c}, \tag{1}$$

where $\sigma_{\mathrm{T}} = 6.65 \times 10^{-25}$ cm^2 is the Thomson cross-section, n_{e} is the electron number denisty, $\boldsymbol{v}$ is the electron peculiar velocity, c is the speed of light and $\hat{\boldsymbol{n}}$ is the observer's line-of-sight toward the LBG (Zel'dovich & Sunyaev 1980). The integration traces the photon's path through the LBG outflow.

The radial extent of the outflow is found by solving the corresponding hydrodynamics equations. These coupled non-linear partial differential equations can be reduced to a single ordinary differential equation (Tegmark, Silk & Evrard 1993; Furlanetto & Loeb 2003) under the assumption that the gas swept up by the outgoing blast wave lies in a thin shell behind the propagating shock front (the so-called *thin shell approximation*). The validity of this approximation is illustrated by the self-similar Sedov–Taylor–von Neumann solution for a point explosion in which 90 per cent of the swept-up mass resides in a shell of thickness 10 per cent of the outflow's radius (see Ostriker & McKee 1988 and Ikeuchi, Tomisaka & Ostriker 1983 for additional discussion on this approximation). The

★E-mail: dbabich@cfa.harvard.edu (DB); aloeb@cfa.harvard.edu (AL)
†Current address: California Institute of Technology, Theoretical Astrophysics, MC 130-33 Pasadena, CA 91125, USA.

thin shell approximation allows us to treat the radiative transfer of CMB photons through the shock front in a plane parallel geometry. When the thickness of the shock front is small compared with the shock front's radius of curvature, the path length through the shock front can be expressed as

$$\delta l \approx \frac{\delta R}{|\hat{\boldsymbol{n}} \cdot \hat{\boldsymbol{v}}|}, \tag{2}$$

where δR is the thickness of the shock front. Using conservation of mass and the density compression ratio for a strong adiabatic shock, one gets $\delta R/R = (\gamma - 1)/(3\gamma + 3)$, where R is the radius of the outflow and γ is the adiabatic index of the gas (Ostriker & McKee 1988).

Within the thin shell approximation, the line-of-sight integration in equation (1) is simplified to

$$\left(\frac{\Delta T}{T}\right)_i = -\frac{\sigma_{\rm T}\,\delta R}{c}[n_{\rm e}(\boldsymbol{r}_1)v(\boldsymbol{r}_1) - n_{\rm e}(\boldsymbol{r}_2)v(\boldsymbol{r}_2)], \tag{3}$$

where $\boldsymbol{r}_1$ and $\boldsymbol{r}_2$ are the location, in a coordinate system centred on the LBG, on the shock front where the line-of-sight respectively enters and exits the shock front. The subscript i labels the contribution from a particular LBG.

If the outflow is spherically symmetric then there is an exact cancellation of the anisotropies produced at the entry and exit points of the line-of-sight through the LBG shock front.[1] However, observations of low-redshift starburst galaxies, which serve as analogs of the higher redshift LBGs, show evidence for highly non-spherical outflow geometries (Martin 1999). It is therefore reasonable to expect that the early stages of LBG outflows, whether they are driven by starburst or quasar activity,[2] would produce CMB anisotropies.

For simplicity, we will assume that the outflow is axisymmetric about some axis $\hat{\boldsymbol{z}}$ (possibly the rotation axis of the galactic disc or possibly the jet axis of a central quasar) and expand both the outflow velocity and shock front density in Legrendre polynomials, $\boldsymbol{v}(\boldsymbol{r}) = \hat{\boldsymbol{r}} \sum_\ell v_\ell(r) P_\ell(\hat{\boldsymbol{z}} \cdot \hat{\boldsymbol{r}})$ and $n_{\rm e}(\boldsymbol{r}) = \sum_\ell n_\ell(r) P_\ell(\hat{\boldsymbol{z}} \cdot \hat{\boldsymbol{r}})$, where we have assumed that the velocity field is radial ($\hat{\boldsymbol{v}} \equiv \hat{\boldsymbol{r}}$). Even if the outflow began highly collimated, it will eventually isotropize as it propagates into the intergalactic medium (IGM; an analogous tendency exists in relativistic flows, see Ayal & Piran 2001). On longer time-scales, IGM inhomogeneities, such as filaments and voids, will once again make the outflows non-spherical. Numerical simulations are needed in order to properly model these effects. Here we parametrize the level of asphericity in the outflow by a coefficient ϵ (see equation 7 below).

The outline of this Letter is as follows. In Section 2 we analyze the CMB anisotropy induced by a single LBG with an arbitrarily non-spherical outflow. In Section 3 we calculate the resulting CMB power spectrum. In Section 4 we present numerical results and in Section 5 we summarize our conclusions. Throughout our discussion, we will assume the *WMAP*3 cosmological model (Spergel et al. 2006).

[1] Note that even if the outflow had a perfect spherical shape, the finite light-crossing time through the outflow would produce a net non-zero signal because the flow parameters are time-dependent. This effect would produce a signal $\sigma_{\rm T} n_{\rm e} R(\Delta v)/c \sim \sigma_{\rm T} n_{\rm e} (dv/dt)\,(R/c)^2$ that is extremely small and is ignored here.

[2] In this Letter we will only include the feedback driven by supernovae. Energy input from quasars will lead to enhancements in the bubble size and outflow velocity [see Furlanetto & Loeb (2001) for a description of quasar outflows].

2 SINGLE LBG SIGNAL

The signal along a given line-of-sight includes contributions from LBGs with different masses, outflow ages, orientations of the outflow symmetry axis and line-of-sight impact parameters. For simplicity, we begin by analyzing the expectation value for LBGs formed at a certain redshift and of certain mass and age. Because the net effect from a single LBG can be either positive or negative we will find that the mean of the signal along a given direction is always zero, but a non-zero variance will be produced due to Poisson fluctuations in a manner equivalent to a random walk. The analysis will be performed separately for the distinct cases where either one or two lines of sight intersect the same LBG outflow.

2.1 One sightline

First we consider the case where one line-of-sight intersects a single LBG outflow. Averaging over symmetry axis orientation and impact parameter, the expectation value of the fractional temperature perturbation is

$$\left\langle \left(\frac{\Delta T}{T}\right)_i \right\rangle = \int {\rm d}^2\hat{\boldsymbol{z}} P(\hat{\boldsymbol{z}}) \int {\rm d}^2\boldsymbol{b} P(b) \left(\frac{\Delta T}{T}\right)_i. \tag{4}$$

Here $\hat{\boldsymbol{z}}$ is the symmetry axis of the outflow and $\boldsymbol{b}$ is the impact parameter at which the line-of-sight enters the LBG (see Fig. 1 for definitions of the variables we use in describing the LBG outflow). We assume uniform probability distributions for the symmetry axis orientation, $P(\hat{\boldsymbol{z}}) = 1/4\pi$, and for the impact parameter, $P(\boldsymbol{b}) = 1/\pi R^2$. Now we change the integration variable from the impact parameter $\boldsymbol{b}$ to the location of entrance point of the line-of-sight into the LBG outflow $\hat{\boldsymbol{r}}$. Thus, the expectation value defined in equation (4) can be written as

$$\left\langle \left(\frac{\Delta T}{T}\right)_i \right\rangle = \int_{4\pi} \frac{{\rm d}^2\hat{\boldsymbol{z}}}{4\pi} \int_{2\pi} \frac{{\rm d}^2\hat{\boldsymbol{r}}}{\pi} \left(\frac{\Delta T}{T}\right)_i, \tag{5}$$

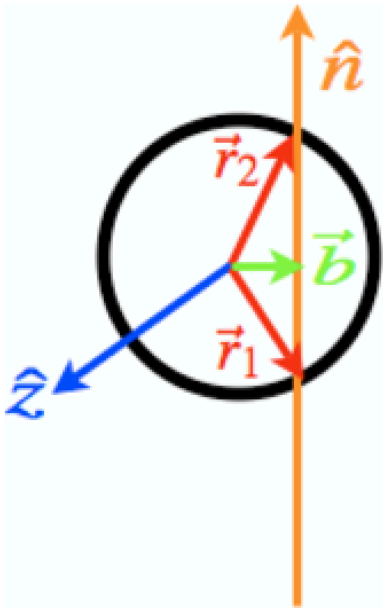

Figure 1. Schematic illustration of the geometry for a single LBG outflow. The black circle represents the shock front, the orange arrow labelled $\hat{\boldsymbol{n}}$ is the line-of-sight from the observer, the red arrows labelled $\boldsymbol{r}_1, \boldsymbol{r}_2$ are the entry and exit points of the line-of-sight on the outflow, the blue arrow labelled z is the symmetry axis of the outflow and the green arrow labelled $\boldsymbol{b}$ is the impact parameter of the line-of-sight.

where the integration over the location of the impact parameter is restricted to a single hemisphere. Performing this integration we find that the signal vanishes on average, as expected from the fact that the net signal for a given LBG is just as likely to be negative as it is to be positive.

There will be a non-zero contribution from a given LBG since the induced anisotropies will be different at the entry and exit points of the line-of-sight through the shock front. Because the LBG symmetry axes is randomly oriented with respect to the direction of the observer, the signal vanishes once the average over this direction is done. This implies that the mean signal and therefore the one-point function vanishes. We are ultimately interested in the two-point correlation function and the related power spectrum. There are two contributions to the power spectrum (Cooray & Sheth 2002). The first is a clustering (two halo) term, originating from the correlated perturbations in the cold dark matter density produced during inflation. The second is a Poisson (one halo) term, originating from Poisson fluctuations in the number density of haloes. The one-point function vanishes because net temperature anisotropy produced by a given LBG is uncorrelated with the signal from other LBGs along the line-of-sight. The clustering term only implies that the number density of LBGs nearby another LBG is greater than average, not that the symmetry axes are somehow correlated.[3] As there is no correlation in the signals between the two distinct lines-of-sight, there will be no contribution to the resulting CMB power spectrum from a clustering term.

2.2 Two sightlines

For a single sightline through each outflow we found that the two-point correlation function vanishes, as the symmetry axes of LBGs are randomly oriented. When both lines-of-sight intersect the same LBG this cancellation does not take place. The average value of the two-point temperature anisotropy when both lines of sight intersect the same LBG is

$$\left\langle \left(\frac{\Delta T}{T}\right)_i^2 \right\rangle = \int \mathrm{d}^2\hat{\boldsymbol{z}} P(\hat{\boldsymbol{z}}) \int \mathrm{d}^2\boldsymbol{b}_1 P(\boldsymbol{b}_1) \int \mathrm{d}^2\boldsymbol{b}_2\ P(\boldsymbol{b}_2) \left(\frac{\Delta T}{T}\right)_i^2 \tag{6}$$

Performing the relevant integrations we find a non-zero answer when the product $n_{\mathrm{e}}(\boldsymbol{r})\, v(\boldsymbol{r})$ has odd parity. The induced fluctuations produced when two lines of sight intersect the same LBG are due to Poisson fluctuations. As mentioned above, we parametrize the deviation from sphericity with a fudge factor ϵ. Then the expectation value for two lines-of-sight intersecting the same LBG outflow region is

$$\left\langle \left(\frac{\Delta T}{T}\right)_i^2 \right\rangle = \sigma_{\mathrm{T}}^2 n_{\mathrm{e}}^2 \delta R^2 \frac{\epsilon^2 v^2}{c^2}. \tag{7}$$

3 POISSON FLUCTUATIONS

We have seen that there is an exact cancellation when the two lines-of-sight intersect two different LBG outflows and that a non-zero signal arises when the two lines-of-sight intersect a single LBG outflow. Correlations in the one-LBG terms are produced by Poisson fluctuations in the number of intercepted LBGs. We will analyze this effect in two stages: first, we will consider the effect along a given line-of-sight (pencil-beam survey) and then generalize to the case of a finite beam size.

3.1 Pencil beam survey

The temperature anisotropies induced by LBGs of halo mass between M and $M + \mathrm{d}M$, formed between redshifts z_{f} and $z_{\mathrm{f}} + \mathrm{d}\, z_{\mathrm{f}}$ and scattering the CMB between redshifts z to $z + \mathrm{d}z$, is

$$\frac{\Delta T}{T} = \sum_{n=1}^{\infty} P_{\mathrm{d}N}(n_{\mathrm{LBG}}) \sum_{i=1}^{n_{\mathrm{LBG}}} \left(\frac{\Delta T}{T}\right)_i, \tag{8}$$

where $P_N(n_{\mathrm{LBG}})$ is the Poisson probability that n_{LBG} LBGs are observed and $\mathrm{d}N$ is the mean number of LBGs in the redshift interval between z and $z + \mathrm{d}z$;

$$\mathrm{d}N = \pi R^2 \frac{-c\mathrm{d}z}{(1+z)H(z)} \frac{\mathrm{d}^2 n}{\mathrm{d}M\ \mathrm{d}z_{\mathrm{f}}}\, \mathrm{d}M\ \mathrm{d}z_{\mathrm{f}}, \tag{9}$$

where R is the radius of an outflow at redshift z produced by an LBG of mass M formed at redshift z_{f}. The total signal is found by integrating over $\mathrm{d}\, M$, $\mathrm{d}\, z_{\mathrm{f}}$ and $\mathrm{d}z$. The expectation value toward a given line of sight vanishes because the expectation value for the temperature anisotropy produced by a single LBG vanishes. Nevertheless, the variance of the signal does not vanish due to Poisson fluctuations. For a single sightline through an LBG outflow region the contribution to the temperature anisotropies can be either positive or negative with equal probability, however for two sightlines the contribution is always non-negative. The resultant variance, which is the case of two sightlines at a separation less than the characteristic angular size of LBG outflows, is

$$\left\langle \left(\frac{\Delta T}{T}\right)^2 \right\rangle = \int \mathrm{d}N \left\langle \left(\frac{\Delta T}{T}\right)_i^2 \right\rangle. \tag{10}$$

The rms value of the anisotropy can be evaluated in terms of the unknowns and the time-changing Legendre coefficients n_ℓ and v_ℓ. For simplicity, we adopt the spherically symmetric solution for the shock radius and velocity, and parametrize the degree of asymmetry in the outflow by the fudge factor ϵ.

3.2 Window function effects

The average angular size of an LBG outflow $\bar{\theta}_{\mathrm{LBG}} \approx 10$ arcsec is below the resolution of the upcoming generation of experiments, and so we must properly account for the beam's window function. The observed temperature anisotropy will be an average over a window function $W(\hat{\boldsymbol{n}})$:

$$\frac{\Delta \tilde{T}}{T}(\hat{\boldsymbol{n}}) = \int \mathrm{d}^2\hat{\boldsymbol{n}}'\ W(\hat{\boldsymbol{n}} - \hat{\boldsymbol{n}}') \frac{\Delta T}{T}(\hat{\boldsymbol{n}}'). \tag{11}$$

For simplicity, we will take the window function shape to be a top hat of angular size θ, namely $W(\hat{\boldsymbol{n}}) = 1/\theta^2$ if $|\hat{\boldsymbol{n}}| \leqslant \theta$, and $W(\hat{\boldsymbol{n}}) = 0$ if $|\hat{\boldsymbol{n}}| > \theta$.

The variance in an angular aperature defined by the window function,

$$\left\langle \left(\frac{\Delta \tilde{T}}{T}\right)^2 \right\rangle_\theta = \int \mathrm{d}^2\hat{\boldsymbol{n}}_1' \mathrm{d}^2\hat{\boldsymbol{n}}_2' W(\hat{\boldsymbol{n}}_1') W(\hat{\boldsymbol{n}}_2') \left\langle \frac{\Delta T}{T}(\hat{\boldsymbol{n}}_1') \frac{\Delta T}{T}(\hat{\boldsymbol{n}}_2') \right\rangle, \tag{12}$$

[3] On small scales, the asphericity of the outflows may be correlated because they propagate into the same inhomgeneous IGM, or because tidal gravitational forces produced correlations in the shapes of nearby galaxies (Mackey, White & Kamionkowski 2002).

which is related to the power spectrum as

$$\frac{\ell(\ell+1)C_\ell}{2\pi} \approx \left\langle \left(\frac{\Delta\tilde{T}}{T}\right)^2 \right\rangle_{\theta=2\pi/\ell}. \quad (13)$$

In order for Poisson fluctuations to give a non-zero result, the two lines of sight $\hat{\boldsymbol{n}}'_1$ and $\hat{\boldsymbol{n}}'_2$ must intersect the same LBG. Therefore they must be separated by less than $\bar{\theta}_{\rm LBG}$. This requirement allows us to evaluate equation (12) as

$$\left\langle \left(\frac{\Delta\tilde{T}}{T}\right)^2 \right\rangle_\theta = \frac{1}{\theta^2}\int {\rm d}N \left[\frac{R}{D_{\rm A}(z)}\right]^2 \left\langle \left(\frac{\Delta T}{T}\right)_i^2 \right\rangle. \quad (14)$$

Note that the Fourier multipole corresponding to $\bar{\theta}_{\rm LBG}$ is $\ell = 2\pi/\bar{\theta}_{\rm LBG}$. Here $D_{\rm A}(z)$ is the angular diameter distance to redshift z.

A broad window function allows for a larger number of LBGs within the beam. The window function is normalized such that it integrates to unity, and so one is observing the fractional fluctuations in the signal as an average over $\theta^2/\theta^2_{\rm LBG}$ independent coherence patches in the beam. This is equivalent to a fractional fluctuation of $1/\sqrt{N}$ as expected from Poisson fluctuations.

4 RESULTS

We numerically solve for the evolution of the shock front in the thin shell approximation (Tegmark et al. 1993; Furlanetto & Loeb 2003), taking into account the effects of the halo gravity and the self gravity of the mass shell, the internal pressure of shocked IGM and the acceleration due to the cosmological constant. When calculating the internal pressure we include Compton cooling, adiabatic cooling, and the addition of shock-heated gas. Initially we assume that a fraction $f_* = 0.1$ of the baryons assembled into the central LBG form stars with a Scalo initial mass function. In this case there is one supernova per 126 $\rm M_\odot$ of star formation (Furlanetto & Loeb 2003). Supernovae characteristically produce 10^{51} erg of energy, but only a small fraction of this energy, $f_{\rm SN}$, couples to the outflow, with the rest being radiated away. We adopt a value of $f_{\rm SN} = 0.01$; see Furlanetto & Loeb (2003) and references within for a more detailed description of our outflow model.

Assuming a Sheth–Tormen mass function (Sheth & Tormen 1999) we include the effects from all possible haloes above the minimum galaxy mass. The lowest galaxy mass is determined by the maximum between the Jeans filtering mass and the cooling mass (dictated by the halo's ability to cool through atomic hydrogen line emission).[4] We allow the LBGs to form between[5] $z = 2$ and $z = 8$. We continue to allow the outflow to evolve until its velocity equals Hubble flow at its radius from the LBG or until $z = 0$. Increasing the upper redshift has little effect on our results because of the higher minimum LBG mass, as well as the higher velocity of the Hubble flow which causes the LBG outflows to merge with the IGM at a relatively earlier time. Decreasing the minimum LBG mass could have a significant effect on our results because the ratio of the initial outflow velocity to the halo escape velocity at the initial radius scales as $v_{\rm init}/v_{\rm esc} \propto M^{-2/9}$. However, in low-mass haloes the star formation time-scale increases and supernova feedback becomes capable of decreasing f_*. Some starburst activity continues to lower redshifts, albeit with a reduced intensity compared to high-redshift star formation; changing the lower redshift from $z_{\rm F} = 2$ to $z_{\rm F} = 1$ would change our results by a factor of 2. Because the observed star formation efficiency decreases with decreasing $z_{\rm F}$, our model, which assumes that star formation and the subsequent supernova feedback only depends on the LBG mass, overestimates this change.

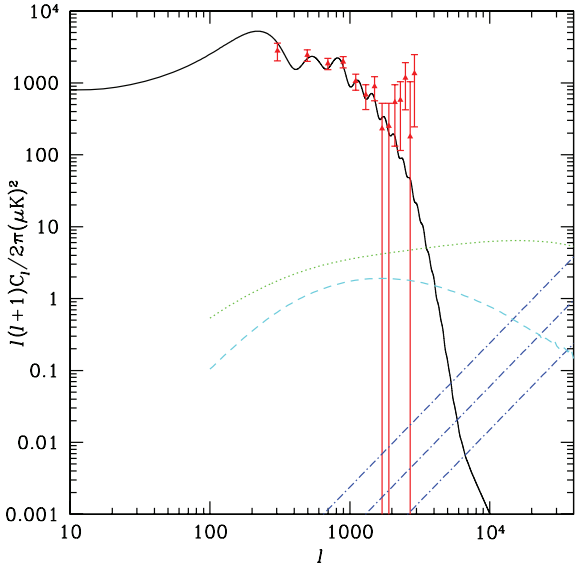

Figure 2. Power spectra produced by several secondary mechanisms. The contribution from the LBG outflow is shown as the three blue dot–dashed curves for $\epsilon = 1$, 0.5 and 0.25 from top to bottom. The primary CMB anisotropies are shown in the solid black curve; the Ostriker–Vishniac and patchy reionization contributions as calculated by McQuinn et al. (2006) are shown by dotted green and dashed light blue lines, respectively. The observed CBI data points are plotted as red triangles.

In Fig. 2 we show the CMB power spectrum produced by several secondary mechanisms. The three blue dot–dashed curves denote the LBG outflow signal calculated in this Letter for the values of $\epsilon = 1, 0.5$ and 0.25 from top to bottom. The green dotted curve delineates the Ostriker–Vishniac effect and the dashed cyan curve describes the patchy reionization effect as calculated by McQuinn et al. (2006)[6] Also, for comparison, we show the primary CMB anisotropies (solid black curve) and the small scale Cosmic Background Imager (CBI) data points (red triangles) (Readhead et al. 2004).

To characterize our results, let us mention some typical quantities for a common LBG halo of mass 5×10^9 $\rm M_\odot$ formed at $z_{\rm F} = 2$. In this case the outflow reaches a maximum comoving radius of 150 kpc at $z = 0.9$ before it merges with the Hubble flow. At late times the outflow velocity with respect to the local Hubble flow is $(v - HR)/c \sim 7 \times 10^{-4}$ and the Thomson scattering optical depth through the shock front is $\tau \approx 10^{-5}$.

These small characteristic values for the Thomson scattering optical depth and outflow velocity imply that the signal should not be notably polarized. Thomson scattering of a radiation field containing a quadrupole moment will produce polarized radiation. There are two standard ways in which scattering by a halo can produce

[4] Note that we include haloes with masses below the observational sensitivity for LBGs, as there is no fundamental reason to exclude these haloes.

[5] We include this lower redshift limit because the phenomenon of downsizing, as well as the evolution of the active galactic nuclei luminosity function, implies that massive galaxies finished forming stars around that redshift.

[6] Note that McQuinn et al. (2006) used a different cosmological model with a higher value of $\sigma_8 = 0.9$. This artificially raises the amplitude of the results compared to value of $\sigma_8 = 0.73$ adopted in this work in line with *WMAP*3.

polarization; (i) photons will double scatter in the halo; (ii) the peculiar velocity of the scatterer will induce a quadrupole moment in the radiation field (Zel'dovich & Sunyaev 1980). In the first case, the radiation can scatter in the halo producing an anisotropic radiation field; a second scattering of that radiation field can produce polarization at the level $\mathcal{O}(\tau^2 v/c)$. In the second case, the peculiar velocity of the scatterer perpendicular to its line-of-sight with respect to the observer will induce a quadrupole in the incident radiation field at the order of $\mathcal{O}(v^2/c^2)$. A fraction τ of the radiation field will scatter and become polarized at the level $\mathcal{O}(\tau v^2/c^2)$. Because values of τ and v/c are so small, we conclude that the polarization power spectrum (which is sixth order in the small parameters of τ and v/c) is negligible.

5 DISCUSSION

The contribution of outflows from Lyman break galaxies to the CMB power-spectrum on arcminute scales is proportional to the square of their characteristic level of deviation from sphericity, ϵ^2. Future CMB experiments could therefore calibrate the intricate feedback process of galactic outflows on the IGM. Most tools used to study these feedback processes focus on the inner few kpc of the LBGs, even though the shock front is typically located at several of tens or hundreds of kpc. The secondary CMB anistropies calculated in this work provide a unique probe of these extended perturbed regions around starburst galaxies at high redshifts.

Even though the amplitude of the power spectrum produced by this effect is small, the signal has distinctive spectral and spatial characteristics. The power spectrum has the same scaling with Fourier multipole ($\propto \ell^2$) as radio or infrared point sources. However, the frequency dependence of the anisotropies produced by our effect has the standard blackbody spectrum, whereas the radio point sources have a power-law frequency spectrum. This distinct feature of our effect may allow future small-scale experiments, many of which have excellent frequency coverage, to separate the anisotropies produced by LBGs from radio point sources.

ACKNOWLEDGMENTS

This work was supported in part by Harvard university grants. DB thanks the Harvard Institute for Theory and Computation for its hospitality when this work was completed, and acknowledges helpful conversations with Re'em Sari and Niayesh Afshordi. We also thank Matt McQuinn for making available the numerical results from his work.

REFERENCES

Ayal S., Piran T., 2001, ApJ, 555, 23
Cooray A., Sheth R., 2002, Phys. Rep., 372, 1
Furlanetto S. R., Loeb A., 2001, ApJ, 556, 619
Furlanetto S. R., Loeb A., 2003, ApJ, 588, 18
Giavalisco M., 2002, ARA&A, 40, 579
Gruzinov A., Hu W., 1998, ApJ, 508, 435
Hu W., 2000, ApJ, 529, 12
Ikeuchi S., Tomisaka K., Ostriker J. P., 1983, ApJ, 265, 583
Kosowsky A., 2003, New Astron. Rev., 47, 939
Lo K. Y., Chiueh T. H., Martin R. N., Ng K.-W., Liang H., Pen U.-L., Ma C.-P., 2005, in Lasenby A. N., Wilkinson A., eds, Proc. IAU Symp. 201, New Cosmological Data and the Values of the Fundamental Parameters. Astron. Soc. Pac., San Francisco, p. 306
Mackey J., White M., Kamionkowski M., 2002, MNRAS, 332, 788
Martin C. L., 1999, ApJ, 513, 156
McQuinn M., Furlanetto S. R., Hernquist L., Zahn O., Zaldarriaga M., 2006, New Astron. Rev., 50, 84
Ostriker J. P., McKee C. F., 1988, Rev. Modern Phys., 60, 1
Ostriker J. P., Vishniac E. T., 1986, ApJ, 306, L51
Readhead A. C. S. et al., 2004, ApJ, 609, 498
Ruhl J. et al., 2004, in Bradford C. M. et al., eds, Proc. SPIE Vol. 5498, Z-Spec: a Broadband Millimeter-Wave Grating Spectrometer: Design, Construction, and First Cryogenic Measurements. SPIE, Bellingham, p. 11
Sheth R. K., Tormen G., 1999, MNRAS, 308, 119
Silk J., 1968, ApJ, 151, 459
Spergel D. N. et al., 2006, ApJ submitted (astro-ph/0603449)
Tegmark M., Silk J., Evrard A., 1993, ApJ, 417, 54
Vishniac E. T., 1987, ApJ, 322, 597
Zahn O., Zaldarriaga M., Hernquist L., McQuinn M., 2005, ApJ, 630, 657
Zel'dovich Y. B., Sunyaev R. A., 1980, Pis. Astron. Zh., 6, 545

This paper has been typeset from a TEX/LATEX file prepared by the author.